Analysis of heat flux partitioning model for copper and SUS304 at low heat flux

Se Hyeon Park [a], HangJin Jo [a,b]
[a]*Division of Advanced Nuclear Engineering, POSTECH, Hyoja-dong, Nam-gu, Pohang, Kyung-buk, South Korea*
[b]*Department of Mechanical Engineering, POSTECH, Hyoja-dong, Nam-gu, Pohang, Kyung-buk, South Korea*
sehyeon@postech.ac.kr

1. Introduction

In thermal industry such as nuclear power plants and chip cooling, boiling is more efficient method of transferring heat compared to the other methods. There are main parameters in boiling. One is the critical heat flux (CHF) representing the safety margin and the other is the heat transfer coefficient (HTC) representing the efficiency. In many industries, a variety of materials are utilized, and heat transfer depends on the materials [1]. The numerous studies have been conducted to understand boiling heat transfer and develop the model [2]. Especially, the dynamics of bubbles play an important role in boiling, and the heat flux partitioning model has been developed considering bubble dynamics [3].

In this study, the bubble dynamics of various materials have been evaluated using a high-speed camera, and based on these, each heat transfer contribution has been understood through a heat flux partitioning model.

2. Experiment

2.1 Sample preparation and characterization

To confirm the effect of material on thermal properties, samples are composed of copper and SUS304. The sample, having size of 41 mm x 30 mm, was mirror-polished and cleaned with acetone and ethanol. As shown in Table 1, the roughness of the samples was similar, thereby, the physical effect can be neglected.

Table 1 Sample characterization

	Copper	SUS304
Density (kg/m^3)	8930	8000
Specific heat (J/kgK)	385	500
Thermal conductivity (W/mK)	398	15
Contact angle (˚)	80	62
Roughness (Ra, μm)	0.14	0.19

2.2 Pool boiling experimental setup and procedure

To use the heat flux partitioning model, an experiment apparatus was designed to conduct pool boiling using high-speed camera (Fig. 1). Under the atmospheric pressure condition, the working fluid was deionized water and saturated. The heat flux and temperature were recorded for 2 min at every step. The high-speed camera was installed horizontally to the sample to measure bubble dynamics (nucleation site density, bubble departure diameter, frequency). As the heat flux increased, the bubble merged and the bubble dynamics could not be measured. Therefore, visualization was conducted only at a low heat flux.

2.3 Uncertainty and data reduction

Assuming conduction has one-dimension, the heat flux was determined as

$$q'' = k_{cu}\frac{dT}{dx} = k_{cu}\frac{dT_{N,2}-dT_{N,1}}{dx_{N,2}-dx_{N,1}}$$

The heat flux depends on the measurement of TC and hole machining of TC. Thus, the uncertainty of heat flux is

$$U_{q''} = \sqrt{\left(\frac{\partial q''}{\partial \Delta T}U_{\Delta T}\right)^2 + \left(\frac{\partial q''}{\partial \Delta x}U_{\Delta x}\right)^2}$$

Uncertainty of heat flux is 2.7% when heat flux is $1MW/m^2$.

The surface temperature is calculated using Fourier's law of conduction as

$$T_{sur} = T_{sub} - q''\frac{L_s}{k_{sample}}$$

The surface temperature depends on the measurement of TC, hole machining of TC and heat flux. Thus, the uncertainty of surface temperature is

$$U_{T_{sur}} = \sqrt{\left(\frac{\partial T_{sur}}{\partial \Delta T}U_{\Delta T}\right)^2 + \left(\frac{\partial T_{sur}}{\partial \Delta x}U_{\Delta x}\right)^2 + \left(\frac{\partial T_{sur}}{\partial q''}U_{q''}\right)^2}$$

When heat flux is $1MW/m^2$, the uncertainty of surface temperature is 3.8%.

The visualization was captured over total 3 seconds with 1500fps using a high-speed camera. The nucleation site density was determined by counting the number of nucleation sites from the images over 1 second, then dividing by the surface area. This measurement was repeated three times (total 3 seconds). The frequency was calculated by averaging ten bubble cycle measurements at each nucleation site. With a time resolution of 0.67ms, it was possible to measure the growth/waiting time. Additionally, the Image J software was utilized to ascertain the spatial resolution by dividing the actual length by the corresponding number of pixels, resulting in 51μm/pixel. This resolution was utilized in determining the bubble departure diameter. The bubble departure diameter was determined by taking measurements for up to 15 bubbles at each step and calculating the average. Due to the complex of the boiling phenomena, bubble exhibits uncertainties of measurement like non-spherical shape and the location of bubble edges. Based on these, there were limitations to capture bubble departure diameter. Thus, the approach of descriptive statistics utilizing the mean value was applied and the error was represented in Fig. 3.

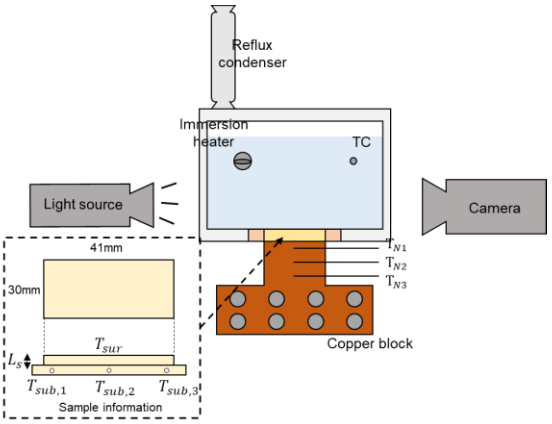

Figure 1. Schematic of pool boiling apparatus and sample

3. Results and discussion

3.1 Boiling performance and bubble dynamics of Copper and SUS304

The results of boiling experiment on copper and SUS304 are shown in Fig. 2. The CHF for copper is 824kW/m^2, and for SUS304 is 576kW/m^2.

The measured boiling parameters are presented in Fig. 3. For nucleation site density and bubble departure diameter, copper had higher values, whereas SUS304 had a longer waiting time.

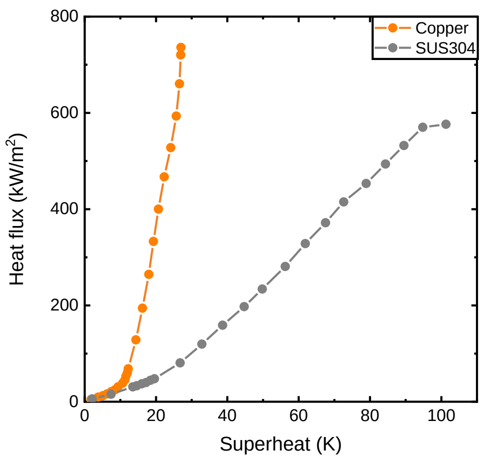

Figure 2. Boiling curve

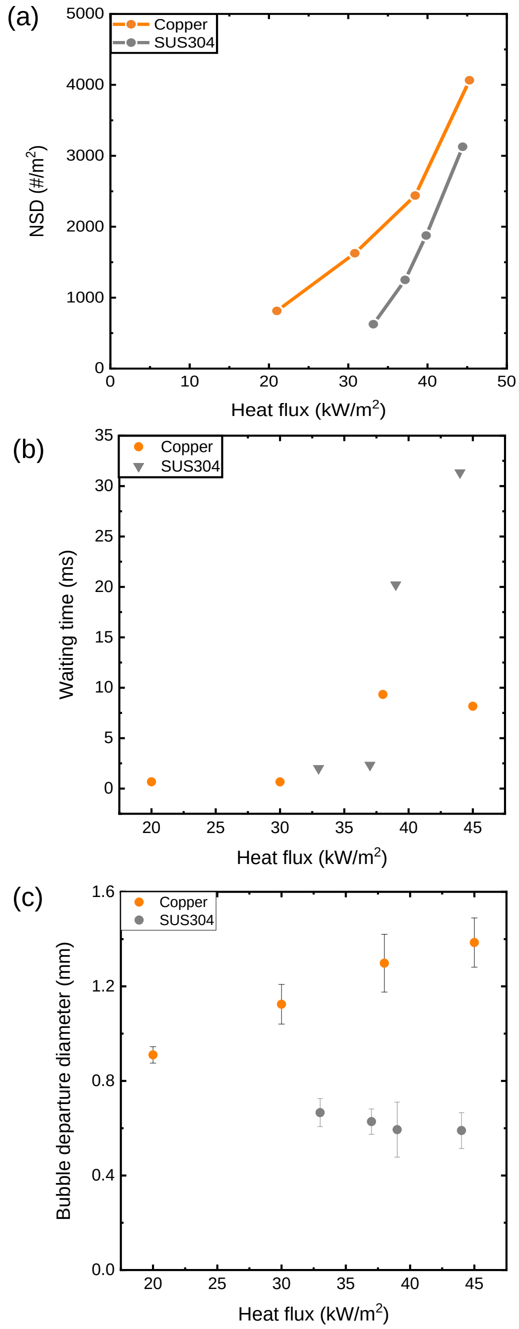

Figure 3. Bubble dynamics of copper and SUS304 (a) Nucleation site density (b) Waiting time (c) Bubble departure diameter

3.2 Heat Flux Partitioning model

To evaluate the contribution of heat transfer in removing heat from the surface, a heat flux partitioning model is used and equation is as follows;

(1) convective heat flux: $q_c'' = h\left(1 - N''\frac{\pi D_b^2}{4}\right)\Delta T$

(2) evaporative heat flux: $q_e'' = N''f\left(\frac{\pi D_b^3}{6}\right)\rho_g h_{fg}$

(3) quenching heat flux: $q_q^{''} = \left(\frac{2}{\sqrt{\pi}}\sqrt{t_w k_f \rho_f c_{p.f}}\right) N^{''} \frac{\pi D_b^2}{4} \Delta T$

Based on the bubble dynamics measured through visualization, the heat flux partitioning model is applied to samples of copper and SUS304, as shown in Fig. 4.

For both samples, the convective heat flux is dominant, followed by quenching heat flux and evaporative heat flux. The reason convective heat flux is the most dominant is that the non-bubble occupies a larger area than bubble at low heat flux. Additionally, as heat flux increases, the area occupied by the bubble enlarges, resulting in an increased quenching heat flux, consistent with previous studies [4,5].

At the same heat flux, the quenching heat flux is higher for copper, which has a larger bubble departure diameter. Specially, copper is 2.3 times greater than SUS304 at 45kW/m^2. This indicates that copper removes more heat than SUS304 during the period between a bubble's removal and reformation, resulting in a lower surface temperature for copper.

Based on this, the bubble dynamics (nucleation site density, bubble departure diameter, waiting time) depend on properties of material and it leads to difference in contribution of heat transfer.

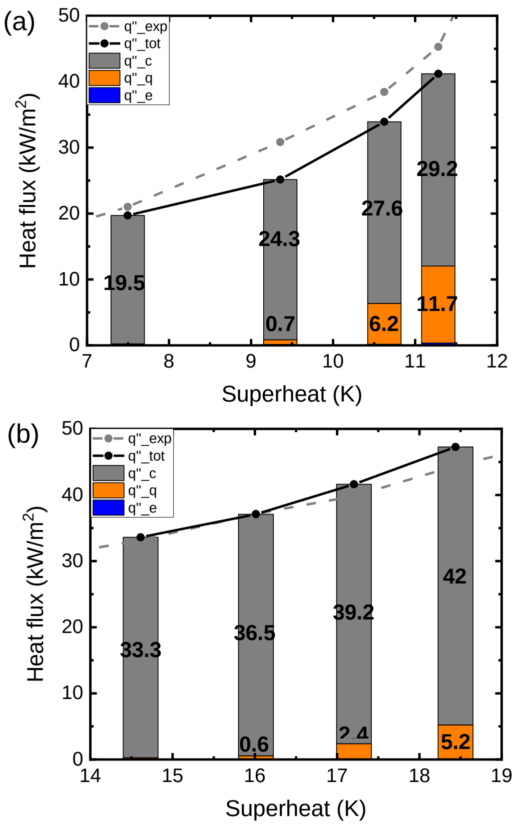

Figure 4. Heat flux partitioning analysis of (a) copper, (b) SUS304

4. Conclusions

This study aims to determine the contribution of heat transfer based on the material. To achieve this, the pool boiling experiment with high-speed camera were conducted on copper and SUS304.

1. When comparing the bubble dynamics, copper had higher values than SUS304 for nucleation site density and bubble departure diameter, while SUS304 had longer waiting time. Based on this, the quenching heat flux is higher for copper than for SUS304
2. For both samples, the convective heat flux was dominant and as heat flux increased, the portion of quenching heat flux enlarged.
3. The bubble dynamics depend on material and result in difference of heat contribution

Acknowledgment

This work was supported by Korea Institute of Energy Technology Evaluation and Planning (KETEP) grant funded by the Korean government (MOTIE). (20222020800130, Development and demonstration of hybrid power system using ORC (Organic Rankine Cycle) and TEG (Thermoelectric Generator) for low and medium temperature industrial waste heat recovery).

REFERENCES

[1] kandlikar, effect of thermophysical properties of the heater
[2] Liang, G., & Mudawar, I. (2018). Pool boiling critical heat flux (CHF)–Part 1: Review of mechanisms, models, and correlations. *International Journal of Heat and Mass Transfer*, *117*, 1352-1367.
[3] Kurul, N., & Podowski, M. Z. (1990). Multidimensional effects in forced convection subcooled boiling. In International Heat Transfer Conference Digital Library. Begel House Inc..
[4] Kim, S. H., Lee, G. C., Kang, J. Y., Moriyama, K., Park, H. S., & Kim, M. H. (2016). Heat flux partitioning analysis of pool boiling on micro structured surface using infrared visualization. International Journal of Heat and Mass Transfer, 102, 756-765.
[5] Gerardi, C., Buongiorno, J., Hu, L. W., & McKrell, T. (2010). Study of bubble growth in water pool boiling through synchronized, infrared thermometry and high-speed video. International Journal of Heat and Mass Transfer, 53(19-20), 4185-4192.